

ROSSI X-RAY TIMING EXPLORER OBSERVATION OF CYGNUS X-1 IN ITS HIGH STATE

W. CUI,¹ W. A. HEINDL,² R. E. ROTHSCHILD,² S. N. ZHANG,³ K. JAHODA,⁴ AND W. FOCKE^{4,5}

Received 1996 July 15; accepted 1996 October 22

ABSTRACT

We present the results from the *Rossi X-Ray Timing Explorer* observations of Cygnus X-1 in its high state. In the energy range of 2–200 keV, the observed X-ray spectrum can be described by a model consisting of a soft blackbody component and a broken power law with a high-energy cutoff. The low-energy spectrum (below ~ 11 keV) varies significantly from observation to observation while the high-energy portion changes little. The X-ray flux varies on all timescales down to milliseconds. The power density spectrum (PDS) can be characterized by excess red noise (“ $1/f$ ”) at low frequencies and a white-noise component that extends to 1–3 Hz before being cut off. At higher frequencies, the PDS becomes power-law again, with a slope of roughly -2 (i.e., “ $1/f^2$ ”). Broad peaks in the range of 3–9 Hz are present and might be due to quasi-periodic oscillations. The PDS shows interesting spectral dependence: the $1/f$ component becomes more prominent when the low-energy spectrum becomes softer. The difference in the observed spectral and timing properties between the low and high states is qualitatively consistent with a simple “fluctuating corona” model.

Subject headings: binaries: general — stars: individual (Cygnus X-1) — X-rays: stars

1. INTRODUCTION

Cygnus X-1 is a prototypical black hole candidate (BHC; see review by Tanaka & Lewin 1995). It spends most of the time in the low (or hard) state, where the soft X-ray luminosity (2–10 keV) is low and the energy spectrum is characterized by a single power law with a photon index of ~ 1.5 (Liang & Nolan 1984). The X-ray flux varies on all timescales down to a few milliseconds, and the power density spectrum (PDS) can be characterized by a flat component with a low-frequency cutoff in the range of ~ 0.04 – 0.4 Hz (see van der Klis 1995 for a review). An additional steepening of the PDS above 10 Hz has also been detected (Belloni & Hasinger 1990). Cyg X-1 has only occasionally been observed in the high (or soft) state (see reviews by Oda 1977 and Liang & Nolan 1984) and is not well studied in such state. In the high state, the power-law photon index varies significantly between 2.6 and 4.2 below 10 keV (Oda 1977) and mildly between 1.6 and 2.3 above 10 keV (Liang & Nolan 1984), while it remains in the range of 1.3–2.3 (above and below 10 keV) in the low state. Therefore it seems as if the hard power-law component exists in both high and low states, but the low-energy (< 10 keV) spectrum becomes much softer in the high state. No PDS has been reported for Cyg X-1 in the high state (van der Klis 1995).

In this Letter, we present the results from the observations of Cyg X-1 in its high state by the *Rossi X-Ray Timing Explorer* (*RXTE*; Bradt, Rothschild, & Swank 1993).

The all-sky monitor (ASM; Levine et al. 1996) light curve of Cyg X-1 revealed that it started a transition from the low state to the high state on 1996 May 10 (Cui 1996; Fig. 1a). During the transition, the soft X-ray flux (1.3–12 keV) increased by roughly a factor of 4, and the ASM hardness ratio, defined as the ratio of the 3–12 keV count rate to that in the 1.3–3 keV

band, shows a steady trend of spectral softening (see Fig. 1b). This trend extends to higher energies. BATSE observations revealed about a factor of 2 decrease in the 20–100 keV flux (Zhang et al. 1996b; Fig. 1c). An anticorrelation between the soft (ASM) and hard (BATSE) X-ray fluxes during the transition, which was observed previously (Dolan et al. 1977; Ling et al. 1987), was firmly established.

Upon the discovery, a series of public Target of Opportunity observations with *RXTE* were carried out to monitor the temporal and spectral variability in the high state. As of 1996 July 15, 12 brief pointed observations of Cyg X-1 have been made with *RXTE*. Here we concentrate on the first four observations. Table 1 summarizes the observation times and durations.

The *RXTE* mission is optimized for observing fast X-ray variability in a broad energy range. For the first time, micro-second timing resolution is achieved for both the proportional counter array (PCA) and High Energy X-ray Timing Experiment (HEXTE) instruments (Bradt et al. 1993), which share a common 1° field of view (FWHM). The PCA has a collecting area of ~ 6500 cm² and covers an energy range from 2 to 60 keV with moderate energy resolution ($\sim 18\%$ at 6 keV). HEXTE has a total effective area of ~ 1600 cm² in two clusters. It covers a wide energy range, from about 15 to 250 keV, with an energy resolution of $\sim 16\%$ at 60 keV.

2. SPECTRAL ANALYSIS

We have taken a conservative approach to spectral modeling since the instrumental calibration is still preliminary. Because of the high intensity of Cyg X-1, we have used Earth-occultation data to estimate the total PCA background. This is adequate because the diffuse X-ray background contributes less than 1% of the source flux below 20 keV, where systematic uncertainties are dominant, and is negligible compared to the instrumental background above 20 keV (Jahoda et al. 1996). A 2% systematic uncertainty has been added to the PCA data to represent uncertainties in the response matrix calibration.

Background subtraction is straightforward for the HEXTE

¹ Center for Space Research, Massachusetts Institute of Technology, Cambridge, MA 02139; cui@space.mit.edu.

² Center for Astrophysics and Space Sciences, University of California, San Diego, La Jolla, CA 92093.

³ NASA Marshall Space Flight Center, Huntsville, AL 35812.

⁴ NASA Goddard Space Flight Center, Greenbelt, MD 20771.

⁵ Also Department of Physics, University of Maryland, College Park, MD 20741.

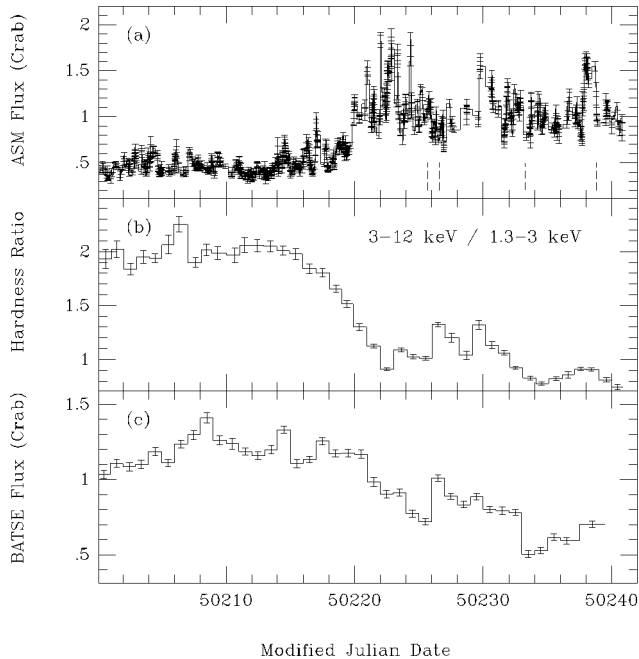


FIG. 1.—(a) ASM light curve of Cyg X-1, comprising measurements from individual “dwells” with 90 s exposure time. The vertical dashed lines indicate when the *RXTE* observations were made. (b) Daily averaged time series of the ASM hardness ratio [(3–12 keV)/(1.3–3 keV)]. (c) Daily averaged BATSE (20–100 keV) light curve. MJD 50213.0 corresponds to 1996 May 10, 00:00:00 UT.

data because the two clusters in HEXTE alternately rock on and off source to provide nearly simultaneous background measurement. However, unmeasured dead-time effects due to large energy losses from charged particles are significant, so we allowed the relative normalization between the PCA and HEXTE to vary during the spectral fitting. We then verified that the resulting relative normalizations were consistent with what we expected from the magnitude of the known dead-time deficit.

The observed X-ray spectrum can be described by a model consisting of a soft blackbody component and a broken power law with a high-energy cutoff. The best-fit model parameters are listed in Table 2. The uncertainties shown represent 90% confidence intervals. Note that, as a consequence of the coupling between the two spectral components at low energies, we derived the uncertainty for the blackbody temperature first, froze it, and then derived the uncertainties for other parameters. The derived N_{H} -value is ~ 20 times larger higher than the interstellar value ($\sim 6.2 \times 10^{21} \text{ cm}^{-2}$; Bałucińska & Hasinger 1991). This could be due to large internal absorption by matter in the binary system. The stellar wind from the supergiant companion may be responsible for providing a large amount of intervening material. However, since we only see the tail of the blackbody spectrum in the PCA energy band, this result can be quite uncertain as a result of systematic uncertainties at the lowest energies. The spectrum was fitted again with N_{H} fixed at the interstellar value, and the results are also shown in Table 2 for comparison. The blackbody component is either not needed or very insignificant in each of the four cases although these fits have consistently higher χ^2 .

Fortunately, Cyg X-1 was also observed by *ASCA* at about the same time as the third *RXTE* observation (Dotani et al. 1996). The *ASCA* spectrum was modeled with a soft blackbody

TABLE 1
RXTE OBSERVATIONS OF CYGNUS X-1

No.	OBSERVATION TIME (UT)	LIVE TIME (s)	
		PCA	HEXTE ^a
1 ...	1996 May 22 17:44:00–19:48:00	4208	1312
2 ...	1996 May 23 14:13:00–18:07:00	7936	5839
3 ...	1996 May 30 07:46:00–08:44:00	2384	2113
4 ...	1996 Jun 4 20:21:00–21:42:00	3280	2415

^a Both clusters are included.

component of temperature $kT = 0.34 \pm 0.02$ keV and a power law with a photon index of 2.4 ± 0.1 (Dotani et al. 1996). Their best-fit N_{H} -value is $\approx 3.2 \times 10^{21} \text{ cm}^{-2}$ (H. Negoro 1996, private communication). These results agree with ours (in the case of low N_{H}) reasonably well (see Table 2).

The results in Table 2 show that the low-energy X-ray spectrum (i.e., α_1) varies significantly in the high state on a timescale of days. Above the break energy (~ 11 keV) the spectral shape changes little. As an example, Figure 2 shows a combined PCA/HEXTE photon spectrum for the first observation.

3. TIMING ANALYSIS

From each of four PCA observations, we chose a contiguous stretch of data 2048 s (or 4096 s) long and generated a PDS in three energy bands: 2–6.5, 6.5–13.1, and 13.1–60 keV. The results were then logarithmically rebinned to reduce scatter at high frequencies. The resulting spectra are shown in Figure 3. The fractional rms amplitude squared is defined as Leahy-normalized power (with Poisson noise power subtracted) divided by the mean source count rate (van der Klis 1995). The PDSs have also been corrected for instrumental artifacts due to electronic dead time and very high energy events (Zhang et al. 1996d). The PDS shows roughly the same shape in different energy bands for a given observation.

In the second observation, the energy spectrum was seen to be the hardest. At this time, the PDS can be characterized by a red-noise component with a characteristic shape of $1/f$ at low frequencies (less than ~ 15 mHz), followed by a white-noise component that extends to ~ 1 Hz, above which it is cut off. At higher frequencies, the PDS becomes power-law again, with a slope of roughly -2 , i.e., “ $1/f^2$.” A broad peak is detected at ~ 3.6 Hz and might be due to quasi-periodic oscillations. When the energy spectrum is softer in the first and third observations, the $1/f$ noise is more significant, and another feature at ~ 9 Hz becomes apparent. Therefore the PDS shows interesting spectral dependence: the $1/f$ component becomes more prominent when the low-energy spectrum becomes softer. The PDS is eventually dominated by the $1/f$ noise in the fourth observation when the energy spectrum is the softest. Similar spectral dependence of the PDS was also observed in another BHC, Nova Muscae 1991 (Miyamoto et al. 1993), and may be common in BHCs. In the last observation, the broad peaks at ~ 3.6 and ~ 9 Hz disappeared, but a fit to the PDS with a broken power law reveals another broad feature that centers at ~ 6 Hz.

4. DISCUSSION

We interpret the soft blackbody component as the emission from a geometrically thin, optically thick cool accretion disk. The soft X-ray photons are Compton upscattered by a geometrically thick, optically thin corona surrounding the disk, to

TABLE 2
RESULTS OF SPECTRAL ANALYSIS

OBSERVATION	N_{H}^{a} (10^{22} cm^{-2})	BLACKBODY	BROKEN POWER LAW ^b		HIGH-ENERGY CUTOFF ^c			χ^2_{ν} /dof	FLUX ^d	f^{e} (%)
		kT_b (keV)	α_1	α_2	E_b (keV)	E_c (keV)	E_f (keV)			
1.....	$11.3^{+1.5}_{-1.8}$	0.27 ± 0.02	$2.95^{+0.04}_{-0.05}$	$1.95^{+0.03}_{-0.04}$	$10.8^{+0.3}_{-0.2}$	24 ± 4	184^{+28}_{-24}	1.00/176	1.88	35
	0.62 (fixed)	...	$2.59^{+0.02}_{-0.01}$	1.86 ± 0.04	10.8 ± 0.3	21^{+3}_{-18}	144^{+19}_{-18}	1.15/179	1.97	...
2.....	$10.0^{+2.0}_{-2.1}$	$0.30^{+0.03}_{-0.02}$	2.60 ± 0.05	1.84 ± 0.02	$11.2^{+0.4}_{-0.3}$	24 ± 2	154 ± 11	1.03/176	1.72	24
	0.62 (fixed)	...	$2.20^{+0.01}_{-0.02}$	$1.79^{+0.03}_{-0.02}$	$12.0^{+0.4}_{-0.5}$	23^{+2}_{-1}	137^{+9}_{-8}	1.55/179	1.80	...
3.....	$10.9^{+1.5}_{-1.6}$	0.27 ± 0.02	$2.98^{+0.05}_{-0.04}$	$1.91^{+0.03}_{-0.04}$	$10.8^{+0.2}_{-0.3}$	25 ± 4	179^{+33}_{-25}	0.83/176	1.38	38
	0.62 (fixed)	$0.30^{+0.11}_{-0.09}$	2.65 ± 0.03	$1.83^{+0.04}_{-0.05}$	10.7 ± 0.3	22 ± 4	141^{+21}_{-18}	0.99/177	1.47	5
4.....	$14.0^{+1.3}_{-1.3}$	$0.24^{+0.02}_{-0.01}$	3.26 ± 0.04	$2.09^{+0.03}_{-0.04}$	10.8 ± 0.2	24 ± 4	216^{+44}_{-32}	0.95/176	1.52	46
	0.62 (fixed)	$0.31^{+0.06}_{-0.07}$	2.82 ± 0.03	1.99 ± 0.04	$10.8^{+0.2}_{-0.3}$	21^{+2}_{-4}	154 ± 22	1.28/177	1.67	9

^a H I column density along the line of sight.

^b Here α_1 and α_2 are soft and hard power-law photon indices, respectively, and E_b is the break energy.

^c E_c is the cutoff energy, and E_f is the e -folding energy.

^d Observed 2–10 keV flux (in units of $10^{-8} \text{ ergs cm}^{-2} \text{ s}^{-1}$).

^e Observed fractional 2–10 keV flux from the blackbody component.

produce the observed hard X-ray emission (Liang & Nolan 1984 and references therein). Then the spectrum can be approximated by a thermal component around the blackbody temperature, a power law (α_1) at energies just above, and a flatter power-law component (α_2) at still higher energies before being cut off beyond kT_e , where T_e is the electron temperature of the corona (Liang & Nolan 1984; see also discussion in Ebisawa et al. 1996). However, the observed high-energy cutoff is so gradual that models with a single electron temperature (e.g., Sunyaev & Titarchuk 1980) fail to fit the high-energy portion of the spectrum. This slow high-energy cutoff can be explained by invoking a stratified hot electron corona (Skibo & Dermer 1995). A similar low-energy spectral shape was observed in the low state by *ASCA* (Ebisawa et al. 1996). In this case, the soft blackbody component had a lower temperature ($kT \approx 0.1 \text{ keV}$), and the broken power law was flatter ($\alpha_1 = 1.92$ and $\alpha_2 = 1.71$), with a lower break energy ($\sim 3.4 \text{ keV}$).

In the high state, the observed PDS shows a distinct $1/f$ component at low frequencies, which was not seen in the low state. This component may be due to the superposition of

random accretion “shots” with long lifetimes (see discussion by Belloni & Hasinger 1990). Theoretical models have been proposed to associate these shots with instabilities in the accretion disk (e.g., Mineshige, Takeuchi, & Nishimori 1994). Perhaps the $1/f$ noise increases its power when the mass

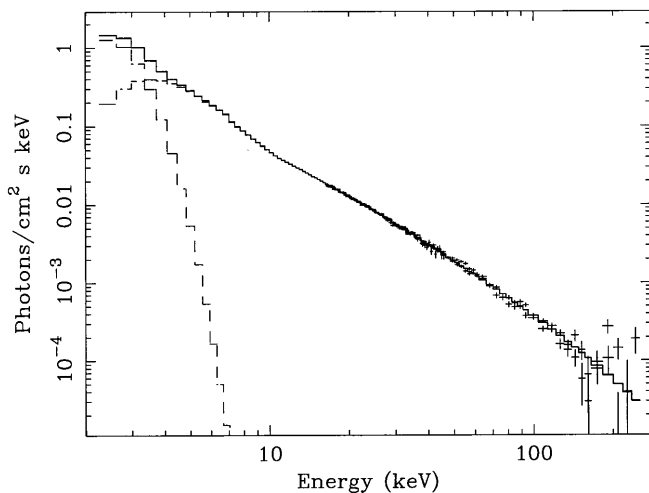


FIG. 2.—Combined PCA/HEXTE photon spectrum of Cyg X-1 for the first observation. For clarity, we show only the Poisson error. The best-fit model is shown by the solid line along with each spectral component in dashed lines, to illustrate their relative contributions.

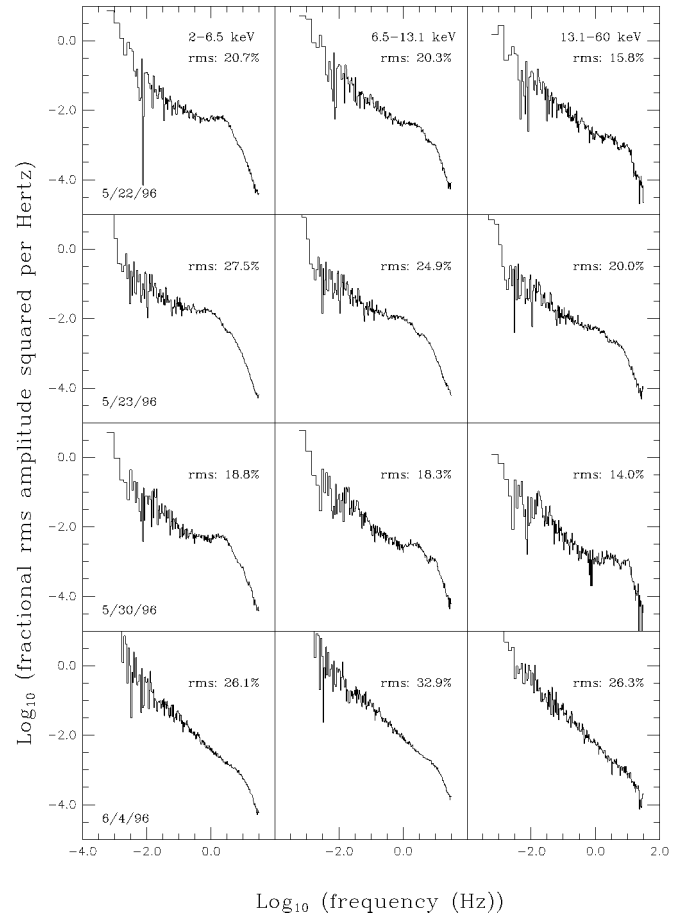


FIG. 3.—Power density spectra in three energy bands derived from the PCA data. The results from different observations are presented in different rows, and each column contains a single energy band. Note that the integrated fractional rms noise shown is derived in the frequency range of 0.488 (or 0.244) mHz to 32 Hz, depending on the observation.

accretion rate is higher, which would explain why it was not observed in the low state (presumably with a lower accretion rate). Its dominance in the fourth observation seems to support this, although there are signs that the bolometric luminosity changes little in going from the low state to the high state (Zhang et al. 1996a). The fourth observation may mark the start of the “true” high state, which is characterized by the soft energy spectrum and dominant $1/f$ noise, following a “settling period.” This is supported by the results from subsequent observations (Cui, Focke, & Swank 1996). Similar power-law PDSs were observed in the soft X-ray transient BHCs Nova Mus 1991 (Miyamoto et al. 1993) and Nova Sco 1994 (Zhang et al. 1996c), in their outburst states, and may be common among BHCs in their high states.

The white-noise (or flat) component has been seen in both high and low states. It may be due to statistical fluctuations in the mass accretion stream near the inner edge of the accretion disk, where the dynamical timescale is very short (compared to the frequency range that has been covered), similar to the “shot noise” in many electronic systems (van der Ziel 1986). The hot corona in the system can act as a low-pass filter that cuts off the white noise at some characteristic frequency to produce the observed “flat-topped” PDS shape. In this model, the cutoff frequency is determined by the characteristic photon escape time. Then the higher cutoff frequency observed in the high state (~ 1 Hz, compared to ~ 0.1 Hz in the low state) can be explained by a smaller corona that is due to more efficient local cooling, provided by a higher mass accretion rate. Because the corona is smaller in the high state, the number of scatterings that an X-ray photon experiences is, on average, less, and therefore the emerging hard X-ray spectrum is softer, which agrees qualitatively with the observations. In the fourth observation, the white noise becomes negligible compared to the $1/f$ noise, and the observed PDS shape is consistent with the $1/f$ noise being cut off at ~ 16 Hz (thus becoming $1/f^2$ at

higher frequencies). Therefore the corona seems to be even smaller in this case, which would explain the softest energy spectrum among all observations (see Table 2).

What is the origin of the broad PDS peaks detected between 3 and 9 Hz? Similar features are often seen in the noise spectra of solid-state devices. They are thought to be produced by a charge generation and recombination process due to the existence of impurities in semiconductor material (van der Ziel 1986). In this case, the noise spectra are characterized by a flat component below a characteristic frequency and a power-law shape of $1/f^2$ above, which is the same as that of exponential accretion “shots” (Belloni & Hasinger 1990). Similar processes might be involved in mass accretion as a consequence of shocks and turbulences in the accretion disk that disrupt the flow. As a result, the lifetime distribution of the accretion shots may not be random, but limited to certain values because of activation or some other critical conditions (see, e.g., Mineshige et al. 1994) in such processes. It seems more likely, however, that these features are related to resonances in the fluctuating corona because they appear to be more prominent at higher energies.

Note added in manuscript.—After we submitted this Letter, we became aware of another paper submitted at about the same time by Belloni et al. (1996), which is based on some of the same data presented here. We have independently reached some similar conclusions. For example, their proposed “intermediate state” is similar to our “settling period.”

We wish to thank every member of the *RXTE* team for the success of the mission. We would like to thank J. Swank and H. Bradt for valuable comments and E. H. Morgan for discussions on timing analysis. We are also grateful to an anonymous referee for comments that resulted in an improved manuscript. This work was supported in part by NASA contracts NAS 5-30612 and NAS 5-30720.

REFERENCES

- Balućńska, M., & Hasinger, G. 1991, *A&A*, 241, 439
 Belloni, T., & Hasinger, G. 1990, *A&A*, 227, L33
 Belloni, T., Méndez, M., van der Klis, M., Hasinger, G., Lewin, W. H. G., & van Paradijs, J. 1996, *ApJ*, 472, L107
 Bradt, H. V., Rothschild, R. E., & Swank, J. H. 1993, *A&AS*, 97, 355
 Cui, W. 1996, *IAU Circ.* 6404
 Cui, W., Focke, W., & Swank, J. 1996, *IAU Circ.* 6439
 Dolan, J. F., Crannell, C. J., Dennis, B. R., Frost, K. J., & Orwig, L. E. 1977, *Nature*, 267, 813
 Dotani, T., Negoro, H., Mitsuda, K., Inoue, H., & Nagase, F. 1996, *IAU Circ.* 6415
 Ebisawa, K., Ueda, Y., Inoue, H., Tanaka, Y., & White, N. E. 1996, *ApJ*, 467, 419
 Jahoda, K., Swank, J. H., Giles, A. B., Stark, M. J., Strohmeyer, T., Zhang, W., & Morgan, E. H. 1996, *Proc. SPIE*, submitted
 Levine, A. M., Bradt, H., Cui, W., Jernigan, J. G., Morgan, E. H., Remillard, R., Shirey, R. E., & Smith, D. A. 1996, *ApJ*, 469, L33
 Liang, E. P., & Nolan, P. L. 1984, *Space Sci. Rev.*, 38, 353
 Ling, J. C., Mahoney, W. A., Wheaton, W. A., & Jacobson, A. S. 1987, *ApJ*, 321, L117
 Miyamoto, S., Iga, S., Kitamoto, S., & Kamado, Y. 1993, *ApJ*, 403, L39
 Mineshige, S., Takeuchi, M., & Nishimori, H. 1994, *ApJ*, 435, L125
 Oda, M. 1977, *Space Sci. Rev.*, 20, 757
 Skibo, J. G., & Dermer, C. D. 1995, *ApJ*, 455, L25
 Sunyaev, R. A., & Titarchuk, L. G. 1980, *A&A*, 86, 121
 Tanaka, Y., & Lewin, W. H. G. 1995, in *X-Ray Binaries*, ed. W. H. G. Lewin, J. van Paradijs, & E. P. J. van den Heuvel (Cambridge: Cambridge Univ. Press), 126
 van der Klis, M. 1995, in *X-Ray Binaries*, ed. W. H. G. Lewin, J. van Paradijs, & E. P. J. van den Heuvel (Cambridge: Cambridge Univ. Press), 252
 van der Ziel, A. 1986, *Noise in Solid State Devices and Circuits* (New York: Wiley)
 Zhang, S. N., Cui, W., Harmon, B. A., Paciesas, W. S., Remillard, R. E., van Paradijs, J., & Yu, W. 1996a, *ApJL*, submitted
 Zhang, S. N., Harmon, B. A., Paciesas, W. S., & Fishman, G. J. 1996b, *IAU Circ.* 6405
 Zhang, S. N., et al. 1996c, *ApJ*, submitted
 Zhang, W., Morgan, E. H., Jahoda, K., Swank, J. H., Strohmeyer, T. E., Jernigan, G., & Klein, R. I. 1996d, *ApJ*, 469, L29